Breakdown of CF_3I Gas and its Mixtures under Lightning Impulse in Coaxial-GIL Geometry

L. Chen, H. Griffiths, A. Haddad
Advanced High Voltage Engineering Research Centre
School of Engineering, Cardiff University
Cardiff CF24 3AA, UK

and **M. S. Kamarudin**
Universiti Tun Hussein Onn Malaysia
Batu Pahat, Johor, 86400, Malaysia

ABSTRACT

SF_6 is widely used in modern transmission and distribution networks because of its outstanding dual qualities: arc quenching and dielectric insulation. As a gas medium, SF_6 is chemically inert, non-toxic, and non-flammable, which makes possible the construction of compact SF_6 switchgear. One major known disadvantage of the gas is that it has a global warming potential which is 23,900 times higher than CO_2. This has led to research into alternative gases with a much lower environmental impact, and one of the emerging candidates is CF_3I. The high boiling temperature of CF_3I means that it has to be used as part of a mixture inside gas-insulated equipment. To carry out the investigation on CF_3I, a scaled-down coaxial system that replicates the maximum electric field of a 400 kV GIL system was designed and fabricated. The insulation performances of CF_3I/CO_2 and CF_3I/N_2 gas mixtures were then examined by measuring the 50% breakdown voltage, U_{50}, using a standard lightning impulse waveform (1.2/50) under absolute pressures of 1 to 4 bar. The experimental results show that CF_3I gas mixtures have promising potential as an insulation medium for application in gas-insulated lines.

Index Terms - Dielectric breakdown, flashover, gas insulated substations, gas insulation, impulse testing, SF_6.

1 INTRODUCTION

THERE is an urgent need worldwide to reduce greenhouse emissions in order to reach the ambitious targets set by governments in response to the Kyoto Protocol on climate change. In high-voltage equipment, such as gas-insulated switchgear (GIS) and gas-insulated lines (GIL), sulphur hexafluoride (SF_6) is the most common dielectric gas besides air. This is because SF_6 is chemically stable with a high arc interruption capability and a dielectric strength around three times higher than air. On the downside, the global warming potential (GWP) of SF_6 over 100 years is 23,900 times that of CO_2 [1].

When investigating suitable SF_6 alternatives, one of the key properties is the dielectric strength, which is controlled by parameters such as electron attachment, electron scattering, and electron ionization [2]. Therefore, highly electronegative compounds containing halogen elements are favoured, since they can recombine quickly.

There are gases which exhibit a higher dielectric strength than SF_6. However, they all possess one or more negative

properties, such as a high boiling point, high GWP, or voltage withstand limitation.

An emerging candidate is trifluoroiodomethane (CF_3I) which has a dielectric strength that is 1.2 times higher than that of SF_6 while possessing a GWP of less than 1 over 100 years. The weak chemical bond C-I in CF_3I means that it can be decomposed quickly in the atmosphere [3]. However, one of the limitations of CF_3I is its high boiling temperature. Furthermore, it has to be used in low proportions as part of a binary mixture with CO_2 or N_2 to reduce the liquefaction temperature. A published report [4], based on the inhalation tests carried out on animals, shows that CF_3I is a slightly toxic gas. The US National Research Council's (NRC) committee on toxicology has recommended that CF_3I has no observed adverse level (NOAEL) on cardiac sensitization if the concentration is 0.2%, whereas the lowest observed adverse level (LOAEL) is at 0.4%. However, CF_3I can only be used as a mixture in high-voltage equipment, thus drastically reducing the overall toxicity of the CF_3I gas mixture.

Experimental investigations have been carried out on CF_3I in the past, mainly in Japan. V-t characteristics were measured using a fast pulse square wave voltage generator with a rise

time of 16 ns for CF_3I and SF_6 [5, 6]. The investigation was carried out for a gap length of 1 cm under atmospheric pressure. The breakdown voltage at 10 μs for CF_3I is 112 kV, which is 27% higher than the 88 kV measured for SF_6. In a more recent paper [7], SF_6 was found to exhibit a much higher breakdown voltage than CF_3I for a gap distance of 2 cm under 0.3 MPa (3 bar abs.).

Several researchers [7-11] have examined the breakdown characteristics of CF_3I/CO_2 and CF_3I/N_2 gas mixtures for non-uniform and uniform electrode configurations. The configuration that has the highest non-uniformity is the needle-plane arrangement with a field utilization factor of 0.025 for a 5 cm gap length. A more uniform field distribution was represented by a plane-plane electrode system. The results revealed that, when the field distribution is highly non-uniform, the dielectric strength of CF_3I is lower than that of SF_6. When the field utilization factor is closer to unity, the dielectric strength of CF_3I outperforms the SF_6 equivalent. Research carried out by Katagiri et al. [12] shows that the interruption capability of the CF_3I/CO_2 gas mixture is far superior to that of CF_3I/N_2 gas mixtures. In [13], the authors investigated the build-up of by-products after 1,300 electrical discharges. The lowest obtained breakdown voltage is 11% lower than the initial value. By-products analysis determined the generation of C_2F_6, C_2F_4, CHF_3, C_3F_8, C_3F_6 and C_3F_5I during the breakdown of CF_3I gas. Electron swarm parameters [14-16] and arc extinguishing capabilities [17] for CF_3I gas mixtures were also investigated through experiments.

The results from the literature indicate that CF_3I may not be a suitable arc quenching gas for GIS applications, which require a high current interruption, due to the build-up of iodine deposition upon every electrical discharge. On the other hand, the insulation capability makes CF_3I a feasible alternative to SF_6 in a GIL system where arc quenching is not a requirement. The field distribution of a GIL can be replicated by a scaled-down coaxial system. There is no previous research on the feasibility of a GIL using CF_3I, and as there are limited data published on CF_3I for a coaxial cylinder configuration [10], a laboratory scaled system was developed for the purpose of experimental analysis. This paper describes the investigation carried out on the scaled-down coaxial GIL system for several CF_3I gas mixtures. The aim is to identify an appropriate CF_3I gas mixture as a suitable candidate to be used for a full-scale 400 kV GIL demonstrator.

2 SCALED GIL DESIGN AND CF₃I GAS PARAMETERS

2.1 DESIGN PRINCIPLE

Existing GIL systems were essentially built from two concentric pipes made of an aluminium alloy and filled with SF_6 or an SF_6/N_2 gas mixture as gas insulation. In a coaxial design, the highest electric field is along the surface of the inner conductor located in the centre of the coaxial geometry where a gas discharge is most likely to occur.

$$E_{max} = U_{applied}/R_a \cdot \ln(R_b/R_a) \qquad (1)$$

Equation (1) [18] can be used to determine the dimensions of the outer conductor inner radius (R_b) and the radius of the

inner conductor (R_a) for the scaled system. This was achieved by replicating an electric field magnitude similar to that found in a 400 kV GIL within the voltage level that can be applied in the laboratory to the system. Selection of 'R_a' and 'R_b' was based on the practical constraints of fitting a scaled system inside the available pressure vessel and the voltage limitation of the high-voltage bushing (approx. 170 kV lightning impulse). Another factor that needs to be taken into consideration is the optimisation of the quantity $\log(R_b/R_a)$ [18], for which a value of unity is considered the optimal ratio of gap distance and field uniformity in a coaxial geometry. By adopting this approach, a maximum electric field strength similar to that of a 400 kV GIL system was achieved with practical values of a = 1 cm, b = 3 cm at an applied voltage of 90 kV. The field utilization factor f of the coaxial GIL system is 0.55, and is calculated by equation (2) [18]

$$f = \frac{R_a \cdot \ln(R_b/R_a)}{R_b - R_a} \qquad (2)$$

The maximum breakdown field strength E_{50} of CF_3I gas mixtures can be combined into a single expression from (1) and (2) as

$$E_{50} = U_{50}/f \cdot (R_b/R_a) \qquad (3)$$

where the U_{50} is 50% breakdown voltage, E_{50} is the maximum breakdown field strength at U_{50}, outer conductor inner radius is 'R_b' and the inner conductor radius is 'R_a'.

2.2 SIMULATION, DESIGN AND FABRICATION

Several features were incorporated into the design: firstly, a curving radius was added onto both ends of the enclosure tube. This ensures that the gap spacing widens as it approaches the end of the enclosure tube, with the gap spacing for the centre region remaining constant. This design feature minimises the end effects and forces the breakdown to occur in the coaxial area along the cylinder centre region that is of interest in this investigation. Secondly, the design ensures a minimal region of contact between metal parts and insulators to avoid the triple junction effect. The dimensions of the scaled system are shown in Figure 1.
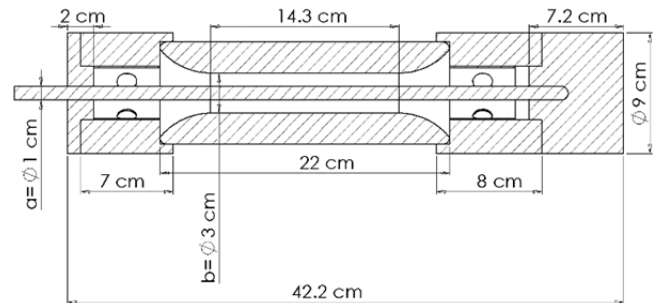

Figure 1. Design of scaled coaxial GIL system. "a" and "b" indicate the diameters corresponding to R_a and R_b.

Numerical finite element simulations were carried out on the coaxial design shown in Figure 1, and the computed field distribution is shown in Figure 2. The detailed numerical simulations of the coaxial system were used to identify high electric stress regions. In Figure 2, the maximum electric field can be observed along the centre region of the conductor. The

inner enclosure wall is flared out at each end. The flaring of the wall achieves widening of the gap distance towards the end of the enclosure, thereby, reducing the likelihood of breakdown on the edges of the enclosure.
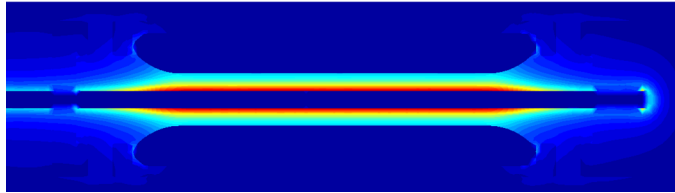
Figure 2. Plot of electric field distribution showing the maximum electric field at the centre of the conductor.

The refined practical system of the scaled coaxial GIL system was fabricated as shown in Figure 3. The enclosure and conductor were both made of aluminium. To keep the two apart, insulators were used to ensure that the conductor was centred inside the enclosure. Gas circulation to the inside of the scaled system was made possible by the holes on the two insulators on both ends. A 1 cm thread was made on the tip of the conductor for attaching the test system onto the high-voltage bushing.
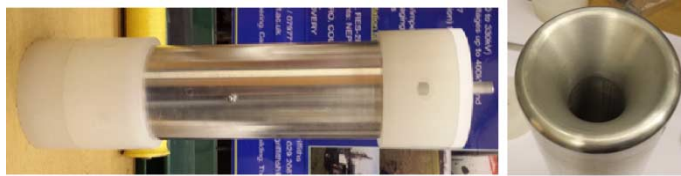
Figure 3. Fully assembled coaxial GIL system. The picture on the right shows the curving radius on the edges of the enclosure wall which reduces end effects.

2.3 SATURATION VAPOUR PRESSURE OF CF$_3$I GAS MIXTURES

Typically, in gas-insulated equipment, SF$_6$ gas is pressurised above 5 bar, which is above the saturation vapour pressure of CF$_3$I, an indication that a buffer gas, such as CO$_2$ or N$_2$, needs to be added. The boiling temperatures of CO$_2$, SF$_6$, CF$_3$I and gas mixtures with 20% and 30% CF$_3$I contents for a pressure range up to 1 MPa (10 bar abs.) are shown in Figure 4.
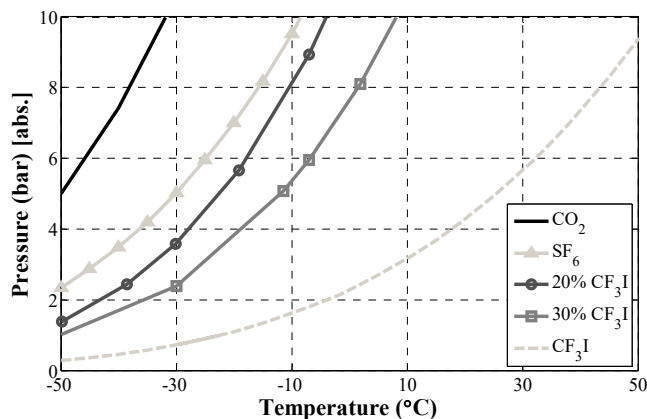
Figure 4. Saturation vapour pressure vs. Temperature curves for SF$_6$, CF$_3$I, CO$_2$, 20% and 30% CF$_3$I content.

The analytical correlation for the saturation vapour pressure of CF$_3$I is given by [19]:

$$\ln (P/P_c) = (A_1\tau + A_2\tau^{1.25} + A_3\tau^3 + A_4\tau^7)T_c/T \qquad (4)$$

where $\tau = 1 - T/T_c$, $A_1 = -7.2$, $A_2 = 1.3$, $A_3 = -1.6$, $A_4 = -5.5$, $T_c = 395$ K and $P_c = 3.9$ MPa.

2.4 CRITICAL FIELD STRENGTH OF CF$_3$I GAS MIXTURES

The effective ionisation coefficients of different gases and gas mixtures were computed using BOLSIG$^+$ software, which applies the two-term approximation of the Boltzmann equation [20]. Here, α is the ionisation coefficient and η is the electron attachment rate. At $(\alpha - \eta) = 0$, the corresponding E/p value represents the critical reduced field strength $(E/p)_{crit}$ for that particular gas or gas mixture, as shown in Figure 5.
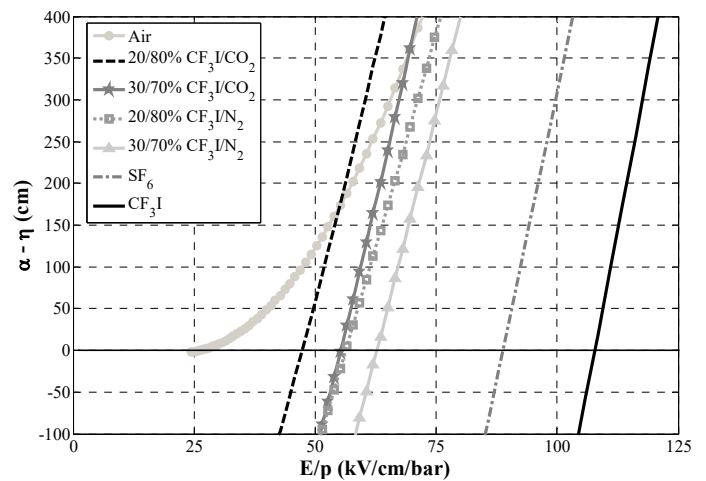
Figure 5. Effective ionisation coefficients in pure gases (air, SF$_6$ and CF$_3$I,) and various CF$_3$I gas mixtures (20/80% and 30/70%).

It can be seen that the $(E/p)_{crit}$ for CF$_3$I at $(\alpha - \eta) = 0$ is 108 kV/cm·bar, whereas SF$_6$ has a $(E/p)_{crit}$ of 89 kV/cm·bar. This is consistent with the results reported in [6], which indicate that pure CF$_3$I has a dielectric strength of around 1.2 times higher than that of SF$_6$. The dielectric strength of CF$_3$I decreases with a lower CF$_3$I content. However, CF$_3$I/N$_2$ gas mixtures have a comparably higher dielectric strength than CF$_3$I/CO$_2$ gas mixtures, as shown in Figure 5. The steepness of the slope for SF$_6$ and CF$_3$I indicates that the two gases are relatively brittle. This means a strong growth of ionisation will occur in the region where E/p > $(E/p)_{crit}$, especially in the presence of defects in the gas-insulated equipment [21]. For a GIL using a CF$_3$I gas mixture, the design requires the interior dimensions to be significantly lower than the $(E/p)_{crit}$ of that particular CF$_3$I gas mixture.

3 TEST SETUP

The experimental investigation was conducted using a 400 kV Haefely impulse generator with a standard lightning waveform of 1.2/50. The aim of this study was to determine a suitable CF$_3$I gas mixture based on breakdown characteristics of the gas mixture.

3.1 LIGHTNING IMPULSE TEST CIRCUIT

Figure 6 shows the circuit diagram of the impulse test circuit. A capacitive voltage divider with a ratio of 27931 to 1 and 50 ns rise time was used in this work to measure the lightning impulse voltage. A digital LeCroy wave-runner 64Xi was used to record the waveform.
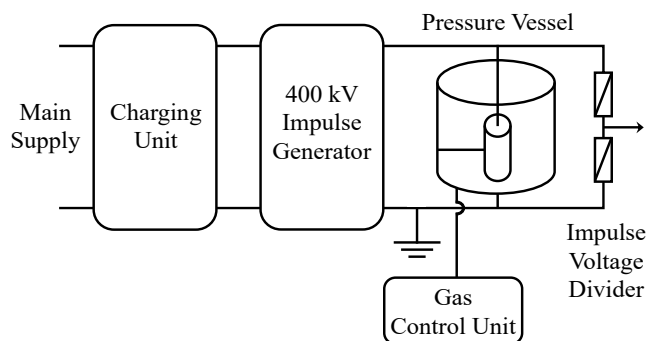

Figure 6. Test circuit diagram of lightning impulse experiment.

3.2 TEST VESSEL AND ITS CONTROLS

In order to carry out the experiment, a pressure vessel (Figure 7a) was manufactured out of mild steel to withstand high gas pressure. The side window was made of polycarbonate; this is a tough thermoplastic material that has a high level of transparency and a suitable material for observing the discharge phenomena occurring inside the vessel. At the bottom of the vessel, there are multiple inlets and outlets for pressurising the vessel and vacuuming out air. A gas removal system (Figure 7b) was also used in the experimental setup, so that CF_3I gas mixtures can be recycled. After each set of tests, the used gas mixture was then transferred into a purposely designed gas storage cylinder.
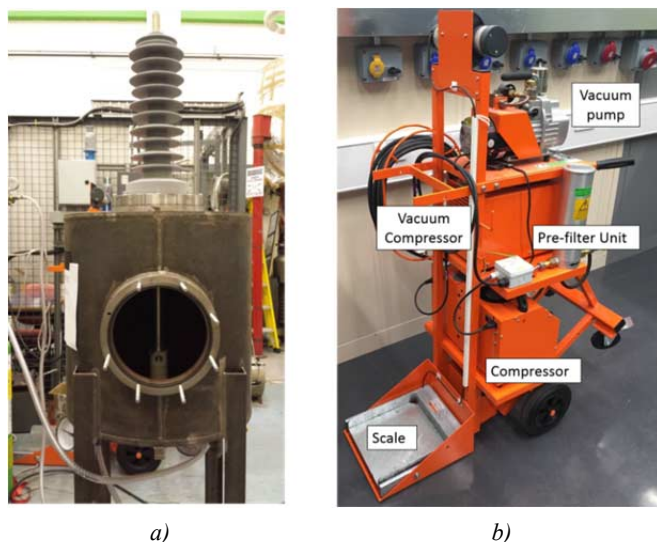

a)   *b)*

Figure 7. Test equipment: a) pressure vessel with coaxial system inside and high-voltage bushing, b) gas removal system for CF_3I gas and its mixtures.

4 BREAKDOWN OF CF₃I MIXTURES IN COAXIAL GEOMETRY

From a practical perspective, a GIL system has two concentric tubes in the form of coaxial cylindrical electrodes. For this experiment, the electrode was mounted concentrically in a vertical position inside the vessel. The breakdown characteristics of various CF_3I/CO_2 and CF_3I/N_2 gas mixtures were investigated using this coaxial system. The aim was to determine an appropriate mixture to be used for application in a full-scale GIL system.

The aim of the present investigation is to obtain the breakdown characteristics of CF_3I gas mixtures tested under different polarities, gap distances and pressures. This required a large number of tests and the up-down method [22] is a testing method that determines the 50% breakdown voltage U_{50} of an electrode configuration within a small number of tests, which requires minimum experimental time and achieves a good level of accuracy. During the experiments, for every test arrangement, a minimum of 30 impulse voltage applications was adopted to provide satisfactory statistical significance.

4.1 EFFECT OF CF₃I CONTENT AND MIXED GAS

Partial pressure of CF_3I in the mixture is generally selected based on a trade-off between three factors: boiling point of the gas mixture, insulation strength, and by-products of the gas mixture following each electrical discharge. Based on these factors, a comparative study was carried out on five CF_3I gas mixtures to investigate their breakdown properties. The results shown in Figure 8 indicate that the mixtures containing CO_2 have a higher breakdown performance than the equivalent CF_3I/N_2 gas mixtures. Initial results obtained at 0.1 MPa (1 bar abs.) have shown a small difference between the 20/80% and 30/70% CF_3I/CO_2 gas mixtures.
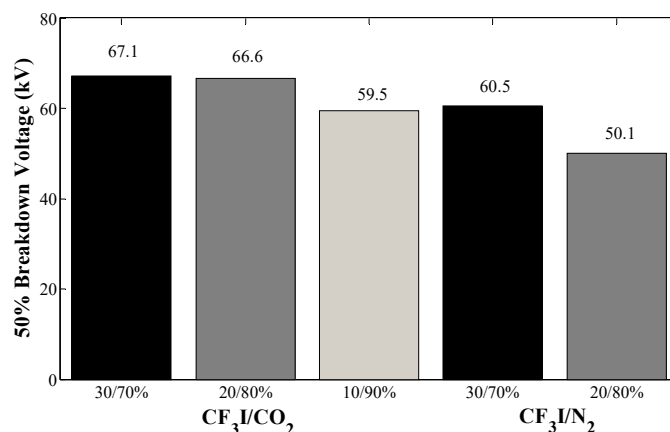

Figure 8. Effects of CF_3I contents and buffer gas on breakdown strength under one pressure bar (abs.) for positive polarity.

4.2 EFFECT OF PRESSURE AND IMPULSE POLARITY

To quantify and gain a better understanding on the effect of pressure and impulse polarity, experiments were carried out over the pressure range from 0.1 to 0.4 MPa (1 to 4 bar abs.) for positive and negative polarities on ratios of 20/80% and 30/70% CF_3I/CO_2 and CF_3I/N_2 gas mixtures.

The breakdown data were then plotted and displayed in Figures 9 and 10 for CF_3I/CO_2 and CF_3I/N_2 gas mixtures respectively. Four observations can be made from these figures: i) the breakdown voltage increases with increasing pressure, ii) higher CF_3I content results in a higher breakdown voltage, iii) the breakdown voltages obtained under positive polarity were higher than their equivalent under negative polarity, and iv) the differences between positive and negative breakdown voltages were smaller for CF_3I/N_2 gas mixtures in comparison with CF_3I/CO_2 gas mixtures.

thereafter, with a gradual decreasing slope. From the $BOLSIG^+$ computations, an estimation of the critical value of $(E/p)_{crit}$ was obtained for different CF_3I gas mixtures. It is expected that, below the $(E/p)_{crit}$, there should be no occurrence of breakdown. However, $(E_{max}/p)_B$ values at higher pressures under negative polarity can be smaller than the critical value of $(E/p)_{crit}$ for CF_3I gas mixtures. This may be attributed to the existence of an electron avalanche with the support of electron emission from the microscopically irregular surface on the cathode.

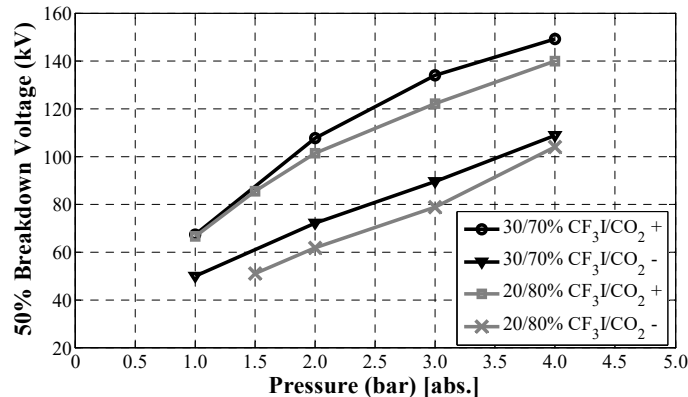**Figure 9.** Breakdown voltage, U_{50}, vs. pressure under positive and negative polarities for various CF_3I/CO_2 gas mixtures.

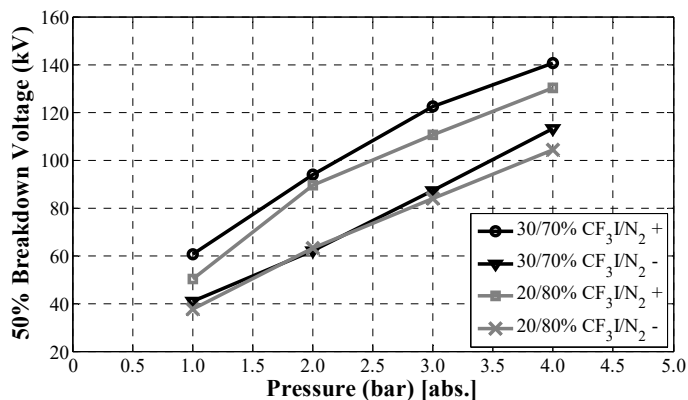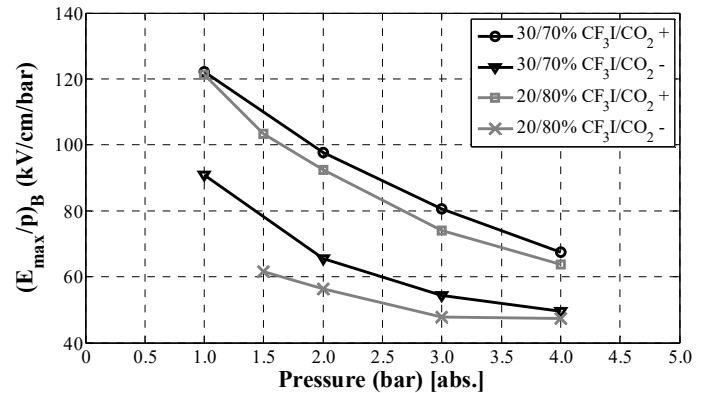**Figure 11.** Characteristics of pressure-normalised maximum field strength for various CF_3I/CO_2 gas mixtures for both positive and negative polarities.

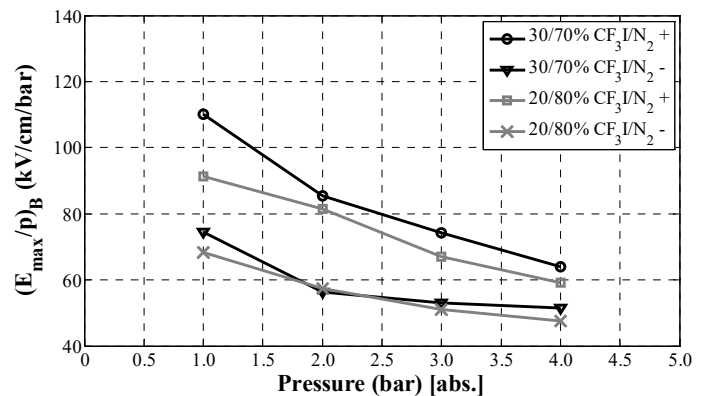**Figure 10.** Breakdown voltage, U_{50}, vs. pressure under positive and negative polarities for various CF_3I/N_2 gas mixtures.

Figure 12. Characteristics of pressure-normalised maximum field strength for various CF_3I/N_2 gas mixtures for both positive and negative polarities.

Furthermore, a polarity effect can be seen in the impulse breakdown voltage results for the coaxial system. As can be observed, the breakdown voltages obtained under negative polarity are much lower than those under positive polarity, particularly at higher pressures. Moreover, the breakdown voltages were shown to be increasing but at decreasing rate as a function of gas pressure up to 4 bar (abs.).

The expression of equation (1) can be rewritten as equation (5) in order to calculate the pressure-normalised maximum field strength at U_{50}, $(E_{max}/p)_B$, for CF_3I gas mixtures. The experimental $(E_{max}/p)_B$ values are shown in Figures 11 and 12 for CF_3I/CO_2 and CF_3I/N_2 gas mixtures respectively.

$$(E_{max}/p)_B = \frac{U_{50}}{R_a \cdot \ln(R_b/R_a) \cdot p} \qquad (5)$$

As can be observed on Figures 11 and 12, the $(E_{max}/p)_B$ decreases with a steep slope in the low pressure range and,

The dielectric strength of CF_3I gas mixtures were then compared with those of SF_6 obtained from published data in the literature. In [23], lightning impulse experiments were carried out on coaxial geometries of 3.2/9.6 cm and 5.0/9.6 cm over the pressure range from 0.1 to 1.5 MPa (1 to 15 bar abs.) under positive and negative polarities.

The 3.2/9.6 cm geometry has the same R_b/R_a ratio as the coaxial system that was investigated in this work, and hence has the same field utilization factor due to the same ratio of R_b/R_a. However, the gap length is different for the two systems, which makes direct comparison on the breakdown voltage not suitable. This has then led to a comparative study using $(E_{max}/p)_B$ values for SF_6 and for the 30/70% gas mixtures of CF_3I/CO_2 and CF_3I/N_2, as shown in Figure 13. It can be observed that, for positive polarity at low pressures, both CF_3I gas mixtures have a higher $(E_{max}/p)_B$ than SF_6 gas and, thereafter, this decreases much more quickly than with SF_6. At 4 bar, the $(E_{max}/p)_B$ of 30/70% CF_3I gas mixture is

around 80% that of SF_6. It can also be seen that, for a CF_3I/CO_2 gas mixture, the $(E_{max}/p)_B$ drops below the $(E/p)_{crit}$ at a much higher pressure than their SF_6 or CF_3I/N_2 equivalent.
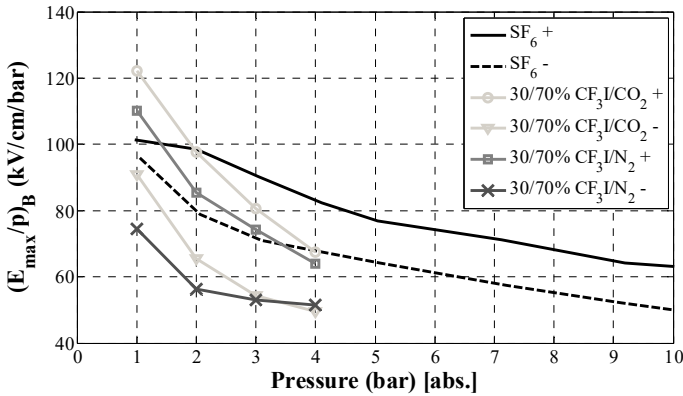
Figure 13. Comparison of pressure-normalised maximum field strength for SF_6, CF_3I/CO_2 and CF_3I/N_2 under positive and negative polarities.

5 BREAKDOWN CHARACTERISTICS OF 30/70% CF₃I/CO₂ GAS MIXTURE

Based on the results shown previously, the 30/70% CF_3I/CO_2 gas mixture has the most promising breakdown characteristics. Breakdown tests were then carried out on the 30/70% CF_3I/CO_2 gas mixture in a coaxial system using different sized inner conductors. The V-t characteristics were also examined under the standard lightning impulse waveform (1.2/50).

5.1 EFFECT OF INNER CONDUCTOR DIAMETER

The enclosure diameter was fixed, and different sized inner conductors were fabricated to investigate the effect of gap spacing in coaxial systems. It was stated in [18] that the highest breakdown voltages can be reached with ratios of R_b/R_a which is very close to the optimum value as shown in Figure 14. It shows that there is a linear relationship between breakdown voltage and pressure irrespective of the gap spacing. However, as pressure increases, the voltage is expected to increase less linearly as found by other researchers for SF_6 gas [24].

An inner conductor with a diameter of 2 cm has a higher geometric uniformity than a 1 cm diameter conductor, hence will lead to a lower breakdown voltage due to the gap spacing between the inner and outer conductors being smaller in diameter. In contrast, a 0.8 cm diameter conductor has a larger gap spacing than a 1 cm diameter conductor, and its associated breakdown voltage is lower due to the geometry exhibiting a more non-uniform field.

Figure 15 shows the $(E_{max}/p)_B$ for the 30/70% CF_3I/CO_2 gas mixture for different sizes of inner conductor under pressures of 1 to 4 bar (abs.). Varying the diameter of the conductors, alters the electric field uniformity, and the measured results suggest that all the curves are saturating near the critical field strength of the 30/70% CF_3I/CO_2 gas mixture at 55 kV/cm·bar. Eventually, the $(E_{max}/p)_B$ values will drop below the critical value $(E/p)_{crit}$ of the CF_3I gas mixture as indicated by the SF_6 data shown in Figure 13 derived from [23].

Two of the coaxial geometries that were investigated in this work had similar geometric ratios to the 3.2/9.6 cm and 5.0/9.6 cm geometries reported in [23] for SF_6 gas. Figure 16 summarises the comparative study carried out in this work. As can be seen on the figure, both sets of coaxial systems have similar trends. The set of systems with a 1/3 ratio (close to optimal) has higher $(E_{max}/p)_B$ values and requires higher pressures to obtain values lower than the $(E/p)_{crit}$. This was expected given the results shown in Figure 14, where a system with a 1/2 ratio has lower breakdown values. The steep slope for the curve $(\alpha - \eta) = 0$ vs. E/p shown in Figure 5 for CF_3I gas and its mixtures indicate the insulation integrity of the gases is precarious near to the $(E/p)_{crit}$. It is, therefore, important to design the GIL system well below the $(E/p)_{crit}$ of the chosen gas mixture to avoid insulation breakdown.
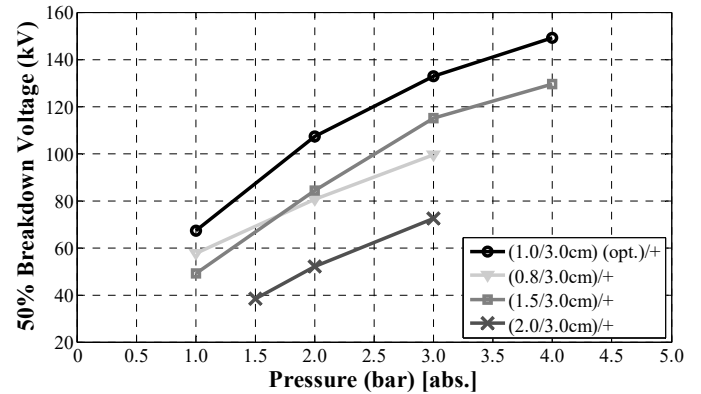
Figure 14. Breakdown voltage, U_{50}, vs. pressure for 30/70% CF_3I/CO_2 gas mixture for different diameters of the inner conductor of the coaxial test configuration.
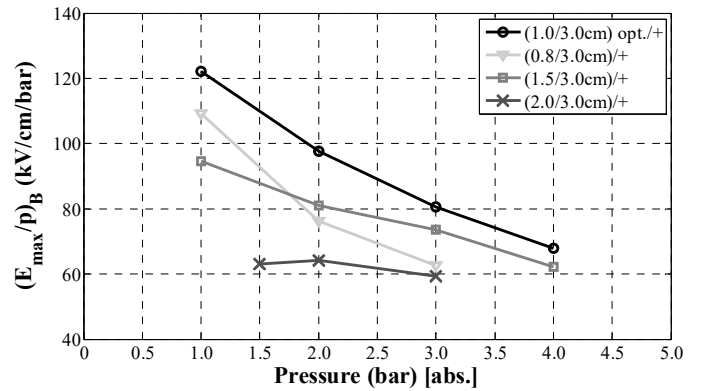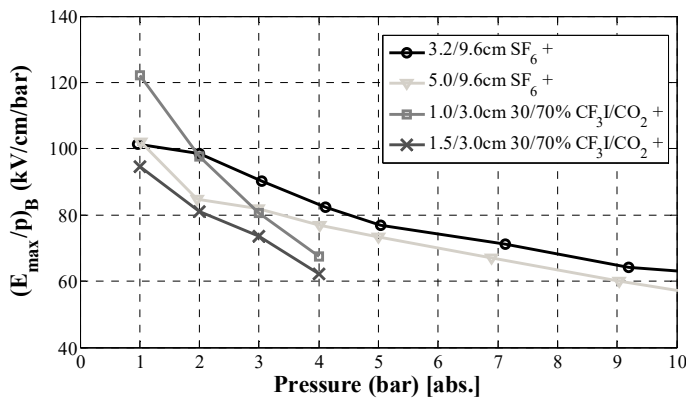

Figure 15. Pressure-normalised maximum field strength, vs. pressure for 30/70% CF_3I/CO_2 gas mixture for different diameters of the inner conductor.

5.2 V-t CHARACTERISTICS

The V-t characteristics for the coaxial geometries were investigated for different CF_3I content, conductor thickness, pressure, and impulse polarity.

Figure 17 shows voltage at time to breakdown $U(T_B)$ as a function of time to breakdown T_B for different CF_3I contents. The value T_B is the sum of statistical (T_s) and formative (T_f) time-lags. There is no clear indication that T_B was affected by changing the CF_3I contents.

In Figure 18, when the pressure was fixed at 3 bar (abs.), the highest breakdown voltage was recorded for 1 cm conductor, which gives a geometric ratio closest to optimal.

Figure 16. Comparison of pressure-normalised maximum field strength vs. pressure for SF_6 and 30/70% CF_3I/CO_2 for two sets of coaxial systems (similar geometric ratios for different radii of the inner conductor in the coaxial test configuration).

The V-t characteristics for the 30/70% CF_3I/CO_2 gas mixture were compared for both positive and negative polarities as shown in Figure 19.

Two common patterns can be observed in Figures 17, 18 and 19: i) fairly flat V-t curves and/or ii) V-t curves rising steeply in the short-time region. The second pattern can be visibly observed at low pressure and small gap spacing.
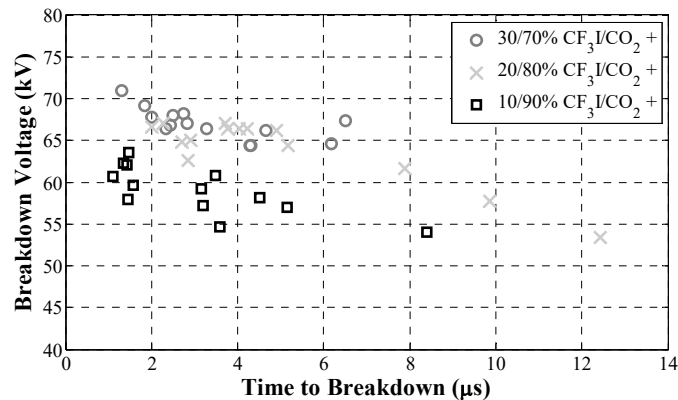
Figure 17. V-t characteristics for various CF_3I/CO_2 gas mixtures: 10/90% 20/80% and 30/70% (1 bar (abs.) and positive polarity).
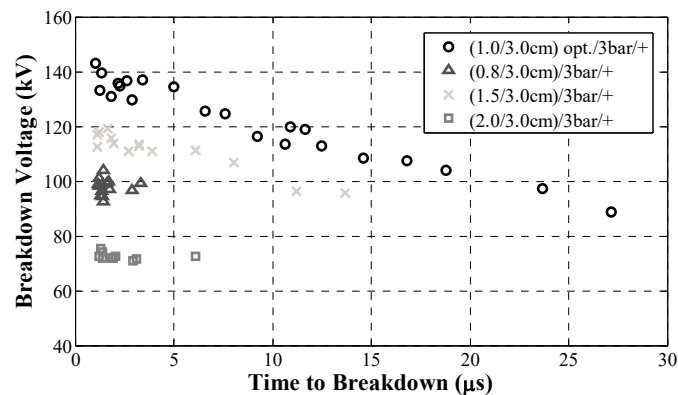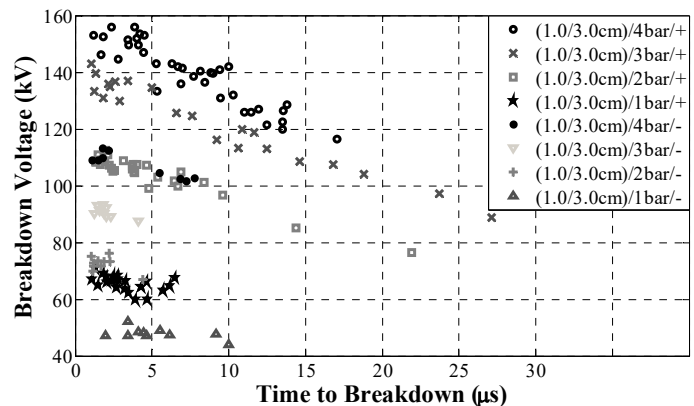

Figure 18. V-t characteristics of 30/70% CF_3I/CO_2 gas mixture for various conductor diameters (3 bar (abs.) and positive polarity).

It was reported in [9] that for a rod-plane configuration, the average T_B for a negative impulse can take longer in comparison to a breakdown for a positive impulse. However,

the results for the coaxial configuration obtained in this work indicate a different behaviour. The breakdown process under positive polarity takes longer, whereas under negative polarity, most of the breakdown events occur in less than 5 μs.

The very divergent high-field region around a rod electrode occupies a small volume of space, so that the T_s for the production of an initiatory electron from natural sources may be long within this restricted volume. In contrast, for the extended geometry of a coaxial electrode, there is a larger volume and more electrons are readily available near the cathode, therefore, a shorter T_s. In the case of a positive rod-plane, ionization is accelerated by electron collision in the high-field region near the rod and complete leaders are formed quickly. For a negative rod-plane, the electrons accelerated into the low-field region by the cathode and in the process become strongly attached to CF_3I. This slows down the ionization process and delayed leaders are formed which may have resulted in longer average T_B for negative breakdowns.

Figure 19. V-t characteristics of 30/70% CF_3I/CO_2 gas mixture under various abs. pressures (positive and negative polarities).

6 CONCLUSION

The breakdown characteristics of CF_3I/CO_2 and CF_3I/N_2 gas mixtures were experimentally investigated in a scaled coaxial system using various sized inner conductors. The obtained laboratory results demonstrate the potential of CF_3I as a candidate to replace SF_6 gas as an insulation medium in high-voltage equipment, particularly in GIL applications.

For the coaxial system, investigations were carried out for CF_3I gas content, buffer gas, pressure, gap length and impulse polarity. In general, increasing the CF_3I content and pressure will result in a higher breakdown voltage. It was found that CF_3I/CO_2 gas mixtures had higher U_{50} in comparison with CF_3I/N_2 gas mixtures. This may have been caused by a poorer synergistic effect between CF_3I and N_2 gases. The polarity effect was present in the coaxial system which may be due to a non-perfect smooth inner surface. The breakdown results were converted into $(E_{max}/p)_B$ and compared with SF_6 results obtained from the literature on coaxial systems with similar geometric ratio. It was demonstrated that for a 30/70% CF_3I gas mixture, the $(E_{max}/p)_B$ value under 4 bar (abs.) pressure is around 80% that of SF_6. Thus, it can be inferred that CF_3I gas and its mixtures have a promising insulation capability, and may be a feasible alternative to SF_6 in a GIL system.

A study was also conducted on the V-t characteristics of CF_3I/CO_2 gas mixtures under a quasi-uniform field distribution represented by the coaxial cylinder configuration. The test results have confirmed that the characteristic depends on the conditions of the gap and the gas pressure. It was found that, on average, the breakdown process for the coaxial geometry under positive polarity takes longer. However, the time to breakdown under negative polarity takes longer for a rod-plane configuration as found in the literature.

To address the various points identified in this work which are not fully explained, tests using a larger scaled coaxial system will be required to further investigate the V-t characteristics of coaxial geometries. The next step of this research is to construct a full-scale 400 kV GIL demonstrator. Extensive testing and optimisation of this system will prove whether CF_3I gas and its mixtures can be used in full practical GIL systems.

ACKNOWLEDGMENTS

REFERENCES

[1] EPA, "Inventory of U.S. Greenhouse Gas Emissions and Sinks: 1990-2000", Office of Atmospheric Programs, U.S. Environmental Protection Agency, Washington, USA, 2002.

[2] L. G. Christophorou, "Insulating Gases", Nuclear Instruments and Methods in Phys. Research, Vol. A268, pp. 424-433, 1988.

[3] L. G. Christophorou and J. K. Olthoff, "Electron Interactions with CF₃I", J. Phys. Chem. Ref. Data, Vol. 29, No. 4, pp. 553-569, 2000.

[4] Subcommittee on Iodotrifluoromethane, Committee on Toxicology, Board on Environmental Studies and Toxicology, Iodotrifluoromethane: Toxicity Review, United States: The National Academies Press, 2004.

[5] H. Toyota, S. Nakauchi, S. Matsuoka, and K. Hidaka, "Voltage-time Characteristics in SF₆ and CF₃I Gas within Non-uniform Electric Field", 14th Int'l. Sympos. High Voltage Eng., H04-466, Beijing, China, 2005.

[6] H. Toyota, S. Matsuoka, and K. Hidaka, "Measurement of Breakdown Voltage and Time Lag Characteristics in CF₃I-N₂ and CF₃I-Air Gas Mixtures by using Steep-front Square Voltage", IEEJ Trans. Fundamentals and Materials, Vol. 125, No. 5, pp. 409-414, 2005.

[7] T. Yagi, T. Maruo, S. Matsuoka, A. Kumada, and K. Hidaka, "Pressure dependence of breakdown voltage under inhomogeneous field in CF₃I gas", IEEJ Trans. Fundamentals and Materials, Vol. 132, No. 8, pp. 700-701, 2012.

[8] S. Nakauchi, D. Tosu, S. Matsuoka, A. Kumada, and K. Hidaka, "Breakdown characteristics measurement of non-uniform field gap in SF₆/N₂, CF₃I/N₂ and CF₃I/CO₂ gas mixtures by using square pulse voltage", 16th Int'l. Conf. Gas Discharges and their Applications, Vol. 2, C-41, pp. 365-368, Xian, China, 2006.

[9] M. S. Kamarudin, A. Haddad, and S. J. MacGregor, "Experimental investigation of CF₃I-CO₂ gas mixtures under lightning impulses", *20th* Int'l. Conf. on Gas Discharges and their Applications, C-4, pp. 370-373, Orleans, France, 2014.

[10] M. S. Kamarudin, L. Chen, P. Widger, K. H. Elnaddab, M. Albano, H. Griffiths, and A. Haddad, "CF₃I Gas and its Mixtures: Potential for Electrical Insulation", CIGRE Session, D1-308, Paris, France, 2014.

[11] M. N. Ngoc, A. Denat, N. Bonifaci, O. Lesaint, W. Daoud, and M. Hassanzadeh, "Electrical breakdown of CF₃I and CF₃I-N₂ gas mixtures", IEEE Conf. Electr. Insul. Dielectr. Phenomena, pp. 557-560, Virginia Beach, USA, 2009.

[12] H. Katagiri, H. Kasuya, H. Mizoguchi, and S. Yanabu, "Investigation of the performance of CF₃I Gas as a Possible Substitute for SF₆", IEEE Trans. Dielectr. Electr. Insul., Vol. 15, No. 5, pp. 1424-1429, 2008.

[13] T. Takeda, S. Matsuoka, A. Kumada, and K. Hidaka, "By-product generation through electrical discharge in CF₃I gas and its effect to insulation characteristics", IEEJ Trans. Power and Energy, Vol. 131, No. 10, pp. 859-864, 2011.

[14] J. de Urquijo, A. M. Juárez, E. Basurto, and J. L. Hernández-Ávila, "Electron impact ionization and attachment, drift velocities and longitudinal diffusion in CF₃I and CF₃I–N₂ mixtures", J. Phys. D: Appl. Phys., Vol. 40, No. 7, pp. 2205-2209, 2007.

[15] M. Kimura and Y. Nakamura, "Electron swarm parameters in CF₃I and a set of electron collision cross sections for the CF₃I molecule", J. Phys. D: Appl. Phys., Vol. 43, No. 14, pp. 5202-5207, 2010.

[16] S. Kawaguchi, K. Satoh, and H. Itoh, "Electron transport in CF₃I and CF₃I-N₂ mixtures", Europ. Phys. J. D, Vol. 68, No. 4, pp. 100-105, 2014.

[17] Y. Yokomizu, R. Ochiai, and T. Matsumura, "Electrical and thermal conductivities of high-temperature CO₂-CF₃I mixture and transient conductance of residual arc during its extinction process", J. Phys. D: Appl. Phys., Vol. 42, No. 21, pp. 5204-5217, 2009.

[18] E. Kuffel, W. S. Zaengl, and J. Kuffel, *High Voltage Engineering - Fundamentals*, 2nd ed., Oxford, UK: Newnes, 2000.

[19] Y.-Y. Duan, M.-S. Zhu, and L.-Z. Han, "Experimental vapor pressure data and a vapor pressure equation for trifluoroiodomethane (CF₃I)", Fluid Phase Equilibria, Vol. 121, No. 1-2, pp. 227-234, 1996.

[20] G. J. M. Hagelaar and L. C. Pitchford, "Solving the Boltzmann equation to obtain electron transport coefficients and rate coefficients for fluid systems", Plasma Sources Sci. Technol., Vol. 14, No. 4, pp. 722-733, 2005.

[21] A. Haddad and D. Warne, "SF₆ insulation systems and their monitoring", *Advances in High Voltage Engineering,* London, UK: IET, Ch. 2, pp. 38-45, 2009.

[22] High-voltage test techniques, BS EN 60060-1, 2010.

[23] S. Menju, H. Aoyagi, K. Takahashi, and H. Qhno, "Dielectric Breakdown of High Pressure SF₆ in Sphere and Coaxial Cylinder Gaps", *IEEE Trans. Power App. Syst.*, Vol. 93, No. 5, pp. 1706-1712, 1974.

[24] T. Takuma, "Discharge Characteristics of Gaseous Dielectrics", IEEE Trans. Dielectr. Electr. Insul., Vol. 21, No. 6, pp. 855-867, 1986.

L. Chen (M'13) obtained a B.Eng. (Hons) degree in Electrical & Electronic Engineering in 2012 and then a Ph.D. in High Voltage Engineering in 2015 from Cardiff University, UK. He is currently working on the characterisation of CF₃I in a gas-insulated line (GIL) demonstrator. His research interests are concerned with the feasibility of replacing SF₆ with an environmentally friendly insulation medium in gas-insulated equipment.

M. S. Kamarudin received his B.Eng. and M.Eng. degrees in Electrical Engineering (Power) from Universiti Teknologi Malaysia (UTM) in 2003 and 2005, respectively and a PhD from Cardiff University, UK, in 2014. Currently, he is a senior lecturer in the Faculty of Electrical and Electronic Engineering at Universiti of Tun Hussein Onn Malaysia (UTHM). His research interests include gas discharges, high voltage surge arresters and dielectrics and electrical insulation systems.

H. Griffiths (M'15) obtained a BSc. degree from the Polytechnic of Wales and a Ph.D. from Cardiff University. Between 1983 and 1990, he worked at the South Wales Electricity Board and the Central Electricity Generating Board in distribution and transmission system design. He is now Professor in the High Voltage Group and at the Petroleum Institute, Abu Dhabi, UAE where he is currently based. His research interests include earthing systems and high voltage insulation. He is a member of a number of BSI, CENELEC, IEC, CIGRE and CIRED working groups and committees. He is a chartered engineer and a member of IET.

A. Haddad (M'13) obtained a first degree in Electrical Engineering in 1985 and then a Ph.D. degree in High Voltage Engineering in 1990. He is now a Professor at Cardiff University. His research interests are in overvoltage protection, insulation systems, insulation coordination and earthing systems. He has published an IET-Power Series Book on "Advances in High Voltage Engineering". He is a member of CIGRE working groups and a member of BSI PEL1/2, IEC TC37. He serves on the scientific committees of several international conferences. He is a Fellow of the IET.